ELSEVIER

Polymer 42 (2001) 667–680

polymer

www.elsevier.nl/locate/polymer

Evidence for a partially ordered component in polyethylene from wide-angle X-ray diffraction

A.M.E. Baker[1], A.H. Windle*

Department of Materials Science and Metallurgy, Pembroke Street, Cambridge, CB2 3QZ, UK

Received 4 February 1999; received in revised form 27 March 2000; accepted 12 April 2000

Abstract

This paper reports a discrepancy found during the analysis of wide-angle X-ray diffraction patterns from a broad range of branched polyethylenes and describes its interpretation. The paper is the second in a sequence of three investigating the structure of polyethylene using new methods in X-ray diffraction and molecular modelling. The X-ray diffraction patterns were recorded from both unoriented and fibre sample forms, using reflection and transmission geometries, respectively. A common set of crystallisation conditions were used to prepare the unoriented samples and the fibre samples were drawn from these unoriented samples using a consistent set of drawing conditions. The X-ray diffraction patterns were fitted to two contributions, namely crystalline and amorphous components, according to standard practice for polymers. However, a discrepancy in crystalline peak positions between low and high angle regions of each diffraction pattern was found for all samples, in both unoriented and fibre forms. The discrepancy is interpreted in terms of an additional distinct contribution to the X-ray diffraction pattern of polyethylene, from a third structural component of intermediate order. The scattering is consistent with partially ordered material and is found to be correlated with not only the branch content but also the branch distribution of the polyethylene. This opens up the possibility of tailoring the influence of the partially ordered component on the polymer's microstructure, and hence properties, by varying the molecular architecture and thermal history. © 2000 Elsevier Science Ltd. All rights reserved.

Keywords: Branched polyethylene; Partially ordered; Third structural component

1. Introduction

Many synthetic thermoplastic polymers are described as semi-crystalline: they show both a melting transition characteristic of crystalline regions and a glass transition characteristic of amorphous (non-crystalline) regions. The microstructure of such semi-crystalline polymers is therefore commonly described by a two component model, of crystalline regions embedded in a matrix of amorphous material. In the crystalline component the polymer chains are by definition highly ordered whilst those in the amorphous component adopt approximately random coil conformations, reminiscent of the polymer in the molten state [1,2]. The two component model has been suggested to be inadequate because the long chain molecules of polymers are unlikely to tolerate the necessary discontinuity in molecular order at the crystal–amorphous boundary [3]. Intuitively a third structural component, an interface of intermediate order, should exist [4] and has been proposed from both theoretical (see for example references 5–7) and experimental (see for example references 8–16) work but crucially not convincingly from the classic structural investigation technique of wide-angle X-ray diffraction. A comprehensive review of the subject, supporting the existence of a third, interfacial component in unoriented, semi-crystalline polymers, has been compiled by Mandelkern [17], citing evidence from a broad range of experimental techniques but wide-angle X-ray diffraction is notably absent. The existence and quantification of a third structural component continues to remain a controversial topic [18–20].

Terms used to describe the suggested third structural component have included semi-ordered, intermediate, rigid amorphous, interfacial, interzonal, interphase and transitional zone. The major theoretical reason for proposing this third component at the crystal–amorphous interface is the instantaneous dissipation of chain flux necessary at the crystallite surfaces where the chains emerge with a high degree of molecular alignment. The chains which emanate from the crystallite surface must either fold back into the

* Corresponding author. Tel.: +44-01223-334321; fax: +44-01223-334300.

E-mail address: ahwl@cus.cam.ac.uk (A.H. Windle).

[1] Present address: MRC Laboratory of Molecular Biology, Hills Road, Cambridge, CB2 2QH, UK.

0032-3861/01/$ - see front matter © 2000 Elsevier Science Ltd. All rights reserved.
PII: S0032-3861(00)00364-5

crystallite, whether by adjacent or non-adjacent re-entry, or must move away from the surface into the amorphous matrix [21]. In the case of melt-crystallisation [22], where the crystallisation conditions are often very far from equilibrium, extensive and perfect chain folding is highly improbable and a proportion of the chains will emerge from the crystallite surface (in polyethylene about 20% of chains have been estimated to show adjacent re-entry [17]). Assuming the crystallites are of infinite extent in the basal plane, then at small distances away from each crystallite surface, most of the chains present will have originated from the crystallite. The average chain orientation here will not be random as in the bulk amorphous matrix but will be distributed around the normal to the crystallite surface: this is the proposed semi-ordered interfacial component. It is conceivable that the thickness of this interface may be influenced by the persistence of the crystalline chain conformation to exist beyond the crystalline environment. In the case of polyethylene, with its planar zig-zag all-*trans* crystalline conformation, this persistence can perhaps be envisaged to be stronger than polymer chains showing a helical crystalline conformation. Nevertheless, even in isotactic polypropylene a third structural component (described as non-crystalline) with a 3_1 helical conformation has been proposed from solid-state ^{13}C NMR spectroscopy [23].

1.1. Unoriented polymers

The techniques which have found experimental evidence for a partially ordered component in unoriented semi-crystalline polymers include electron microscopy after etching or staining [14,15], differential scanning calorimetry [24,25], dielectric relaxation and dynamic mechanical studies [26], small angle X-ray diffraction [8,9,27], solid-state nuclear magnetic resonance (NMR) spectroscopy [12,13,28,29] and Raman spectroscopy [10,11,30,31]. Spectroscopic studies have provided most of the evidence. In addition the discrepancies in crystallinity values determined from different techniques have been attributed in part to values from certain techniques including a contribution from a semi-ordered interfacial region. For example, the higher crystallinity values calculated in branched polyethylenes by density measurements than by calorimetry are attributed to a semi-ordered interfacial region being included in density measurements of crystallinity but not in calorimetry measurements [24]. In another example, incompatible crystallinities reported in different grades of polyethylene from small-angle X-ray scattering (SAXS) and from wide-angle X-ray scattering (WAXS) were reconciled by proposing that a transition layer contributed to the crystallinity value obtained by SAXS but not to the crystallinity value obtained from WAXS [32].

In NMR spectroscopy, three structural components (or even 4 [33,34]) are reported to be needed to account for the observed spectra and the distribution of spin–lattice relaxation times [12,13,29,35–37]. In Raman spectroscopy it has been stated that the spectra of polyethylene cannot be synthesised by weighted sums of the spectra from a model crystalline material (a paraffin) and a model amorphous material (assumed to be molten polyethylene) [10]. The difference spectrum which remains is proposed to originate from a third structural component and is consistent with an intermediate degree of order [10,11,30,38]. Raman spectroscopy is used routinely to quantify the proportion of the third component in polyethylene although recently the method has been called into doubt [18]. The issue remains controversial [19,20].

Estimates of the thickness and proportion of the semi-ordered interface in polyethylene have been made. Thickness values have varied from 10 Å [5,24] to around 30 Å [12] and the proportion from 6 wt% (lightly branched polyethylene) to 20 wt% (highly branched polyethylene) [30,39,40]. The thickness is thought to vary with molecular weight and its distribution and also crystallisation conditions [17,41]. Regarding the nature of the third component, it has been proposed from both solid-state ^{13}C NMR studies [13,33,36] and Raman spectroscopy [10,38] that it consists of *trans* methylene sequences which have lost lateral order but retained an approximately planar zig-zag conformation, consistent with the hypothesis outlined earlier.

The evidence described so far favouring the existence of a third structural component of intermediate order in unoriented semi-crystalline polymers has not included evidence from the classic structural investigation technique of wide-angle X-ray diffraction. If such a component exists in a polymer, its scattering must be contained in the X-ray diffraction pattern. Yet diffraction patterns from polymers are routinely fitted, apparently satisfactorily, to two components: a broad peak(s) corresponding to the amorphous scattering [2] and several sharp peaks corresponding to the crystalline scattering [42]. Disorder parameters have been fitted to X-ray diffraction data [43] but a scattering contribution consistent with degrees of order intermediate between those of the crystalline and amorphous components has not been identified. Opinions to reconcile this discrepancy vary widely, suggesting that the partially ordered scattering is included either with the crystalline [13,36] or the amorphous [34,44] scattering. These explanations are unrealistic, however, since the X-ray diffraction intensity profiles from a third component of partial order must necessarily be intermediate in breadth between those of the sharp crystalline peaks and broad amorphous halo.

The location of the proposed third component within the X-ray diffraction pattern of a polymer has been investigated by McFaddin et al. [44]. The study compared the position of the main amorphous halo in several polyethylenes with the position of the maximum in the scattered intensity profile from molten alkanes, over the temperature range 20–140°C and diffraction angle range 10–34°2θ (CuKα radiation). In polymers, the main amorphous scattering contribution, from interchain interactions, usually occurs just below 20°2θ; a

contribution at higher angles, from intrachain interactions, is often too weak to detect [2,45,46]. At any particular temperature, it was supposed [44] that the molten and therefore non-crystalline alkane chains were random coils and were representative in diffraction terms (peak position) of the truly amorphous component in the solid polyethylenes at the same temperature. It was found, however, that the maximum in scattered intensity from the molten alkanes always occurred at a lower 2θ angle (larger interchain spacing) than the amorphous halo in the solid polyethylenes. This was taken to indicate that not all of the material within the envelope of the amorphous halo of polyethylene is truly randomly packed: some of the chains were proposed to be better packed i.e. partially ordered. The polyethylene diffraction patterns were then refitted, forcing the amorphous halo to occur at the lower Bragg angle calculated from the molten alkane data (19.4°2θ at 20°C by extrapolation) and fitting an extra peak at a slightly higher angle to account for the better packed material. The extra peak representing the 'better packed' material was indistinguishable in width from the amorphous peak and weaker in intensity. This similarity in width between the two peaks was not compatible with the proposed different degrees of order: the improved packing in a partially ordered component should reduce the diffraction peak width relative to the non-crystalline component so that the peak is intermediate in width between the non-crystalline and crystalline peaks, consistent with an intermediate degree of order. Furthermore, the fits which assumed just amorphous and crystalline components were adequate: the introduction of an extra peak in the fitting routine for a partially ordered component did not noticeably further improve the fit and was therefore not justified. Finally, at any given temperature it is not clear that chains in a molten alkane and their diffraction peak position should be representative of chains in a solid polyethylene (different states, densities).

1.2. Uniaxially oriented polymers

The microstructure of semi-crystalline polymers after uniaxial drawing is not thought to be related directly to that before drawing (except perhaps for low draw ratios and drawing at temperatures approaching the melting point) although the exact effects of drawing still remain controversial [46–50]. In highly oriented, semi-crystalline polymers, especially those which have been cold-drawn, a third structural component distinct from crystalline and amorphous material is more widely accepted to exist than in unoriented samples. However, this material is proposed to arise largely from partial orientation of some of the amorphous material during drawing and hence terms used to describe the component in fibres have included oriented mobile and oriented amorphous material. It therefore appears different in origin from the third component in unoriented polymers which is proposed to exist at the crystal–amorphous interface. At low to intermediate draw ratios and drawing performed at temperatures approaching the melting point, the origin of any material described as partially ordered is likely to be difficult to ascertain.

As for unoriented polymers, the experimental evidence for a third structural component in oriented polymer fibres is based largely on spectroscopic studies: for polyethylene, solid-state ^{13}C NMR [35,51–54] and Raman spectroscopy [55,56]. Unlike unoriented polymers, however, strong evidence has also been found from wide-angle X-ray diffraction [57–59]. The proportion of the semi-ordered component in fibres is generally estimated to be higher than in unoriented polymers. For example, it has been estimated to be 34% in polyethylene fibres [54] compared with typical values around 10% in unoriented polyethylene [11].

The evidence from wide-angle X-ray diffraction for an intermediate structural component in fibres originates from studies of polyethylene terephthalate (PET) fibres [57,58] and highly drawn gel-spun polyethylene fibres of ultrahigh molecular mass [59]. The source of most of this component in each case was proposed to be oriented amorphous material between the fibrils as opposed to crystal–amorphous interfaces. For the PET fibres [57,58], the third structural component was proposed after subtraction of the crystalline scattering from the X-ray diffraction pattern failed to reveal the isotropic scattering expected for truly amorphous material. After further subtraction of an isotropic scattering component, the resulting scattering (containing both equatorial and off-equatorial contributions) was described as similar to the scattering obtained from a mesomorphic form of PET [60,61]. This mesomorphic form shows a monoclinic structure where the phenylene rings are thought to be side-by-side, unlike the normal triclinic crystal structure [62]. In the polyethylene study [59], a different form of intermediate, oriented component was proposed because no equatorial scattering contributions were noted, only the (002) and (004) meridional reflections with higher than expected intensities. The component was not observed in typical high molecular weight polyethylene fibres but only in fibres drawn from ultrahigh molecular weight material. The chains of the intermediate phase were proposed to have a mesophase structure with a largely all-*trans* conformation, to be oriented preferentially parallel to the fibre axis but disordered laterally and to be distinct from taut tie molecules [55,63]. An earlier X-ray diffraction study [64] of one of the polyethylene fibres used had also been unable to fit the diffraction pattern satisfactorily to the expected crystal structure [42]. Additional sites with fractional occupancies were introduced into the orthorhombic unit of polyethylene, retaining the two-component model; the later investigation of the same fibre [59] proposed a separate third component.

This paper describes a discrepancy found during analysis and fitting of wide-angle X-ray diffraction patterns from a broad range of polyethylenes in both unoriented and oriented forms. The discrepancy is found consistently in all patterns and is interpreted in terms of scattering from a

third structural component of intermediate order. A similar discrepancy has been noted briefly before [65], as discussed later, although it could not at the time be explained by the authors and was attributed tentatively to stacking faults. The report by Howard and Crist [65] not only provides independent verification of the phenomenon but furthermore is also consistent with our interpretation of the presence of partially ordered material.

This paper is the second in an accompanying sequence of three investigating the structure of a series of branched polyethylenes. The first associated paper [66] describes the structural characterisation of the fifteen commercial grades, including the effects of branch type, concentration and distribution on the crystalline unit cell parameters. The third paper [67] investigates the location of the short chain branches by combining X-ray diffraction and molecular modelling studies. Changes are detected in the values of certain reflection intensity ratios in the X-ray diffraction patterns and shown from molecular modelling to be consistent with inclusion of the branches into the crystalline component, but only to a limited extent. Together the sequence presents a comprehensive and original examination of the structure of branched polyethylene, using new methods in X-ray diffraction pattern recording and analysis and molecular modelling.

2. Methods

Full details of the samples, the preparation techniques used and the X-ray diffraction methods are given in the preceding associated paper [66]. An outline follows here.

2.1. Materials

Fifteen grades of commercial polyethylene were examined which had been well characterised, particularly in terms of branching. The materials were three grades of homopolymer HDPE (high density polyethylene), two grades of methyl-branched HDPE, two grades of LDPE (low density polyethylene), seven grades of LLDPE (linear low density polyethylene) and one grade of VLDPE (very low density polyethylene). The branch contents ranged from fewer than 1 SCB/1000C (short chain branches per 1000 carbon atoms) for the homopolymers (and assumed to be 0 SCB/1000C) to 31 SCB/1000C (12 wt%) for the VLDPE. The branch types ranged from methyl to hexyl. The distribution of branch placements for the LLDPE and VLDPE grades were described by the parameter $\bar{N}_w/\bar{N}_n$ determined from analysis of analytical temperature rising elution fractionation (TREF) data [68]. The possible values of $\bar{N}_w/\bar{N}_n$ range from 1.0 (indicating uniform placement of branches along the chain backbones) up through 1.1 to 1.3 (random placement of branches) to higher values which indicate increasing levels of heterogeneity in branch distribution [69]. The $\bar{N}_w/\bar{N}_n$ values from the eight grades of LLDPE and VLDPE were in the range 1.36 to 1.92; three grades could be described as approximately random in branch placement and five grades as heterogeneous. Full sample details are given in Table 1 of the preceding associated paper [66].

The unoriented samples were prepared by hot-pressing, with a cooling rate of 15°C min^{-1}, to a thickness of either 1.05 ± 0.03 or 0.80 ± 0.03 mm. Uniaxially oriented fibres were drawn from these unoriented samples to a draw ratio of 10, at a temperature of about 40°C below the melting temperature i.e. between 75 and 90°C depending on the branch content. This consistency in sample preparation allowed confidence that any variations observed between the structures would relate primarily to chemical differences between the materials, such as the branching, rather than to differences in thermal treatment.

2.2. X-ray diffraction from unoriented (powder) samples

Fourteen of the 15 polyethylene grades were examined by X-ray diffraction in unoriented form. The X-ray diffraction patterns were recorded in reflection mode at 40 kV, 40 mA from a Siemens D500 $\theta/2\theta$ vertical diffractometer with 2.2 kW sealed tube source (copper target) and parafocusing geometry. Secondary Soller slits and a secondary beam monochromator were used. The slits used were a divergence slit of 0.3°; two anti-scatter slits of 0.3° and a receiving slit of 0.15°. Primary Soller slits were additionally used in some data sets in an attempt to maximise resolution although no significant improvement was noted. A step size of either $0.10°2\theta$ or $0.05°2\theta$ was used. Diffraction data were collected from 18 reflections in the range $10–60°2\theta$.

Correction for sample transparency is rarely made in X-ray diffraction studies but for polymers it is a potential source of considerable error because of their low linear absorption coefficients. A sample transparency correction [70] was applied here on a point-by-point basis, followed by Lorentz and polarisation correction factors, prior to whole pattern fitting structural refinement by the Rietveld method [71,72] using Philips PC Rietveld Plus v1.1B [73]. Fig. A1 in the preceding paper [66] shows the relative importance of these three correction factors under the conditions used here: it is seen that the transparency correction was comparable in importance to the polarisation correction. Diffraction peaks were fitted in the range $10–60°2\theta$ using pseudo-Voigt profiles, including contributions from the $\text{CuK}\alpha_1$ and $\text{CuK}\alpha_2$ wavelength components. The Rietveld method fitted the positions of all peaks to a single set of unit cell parameters. Peak widths were fitted using the Cagliotti equation. It was not found necessary to refine the atomic coordinates of polyethylene [42]. The amorphous scattering was fitted to two broad peaks, one from interchain interactions, at $19.6°2\theta$ and the other from intrachain interactions, at $42°2\theta$ [2]. A background of the form $y_{ib} = c + k\theta_i^2$ was fitted. The March model [74] was used to account for preferred orientation which was found to be present to a

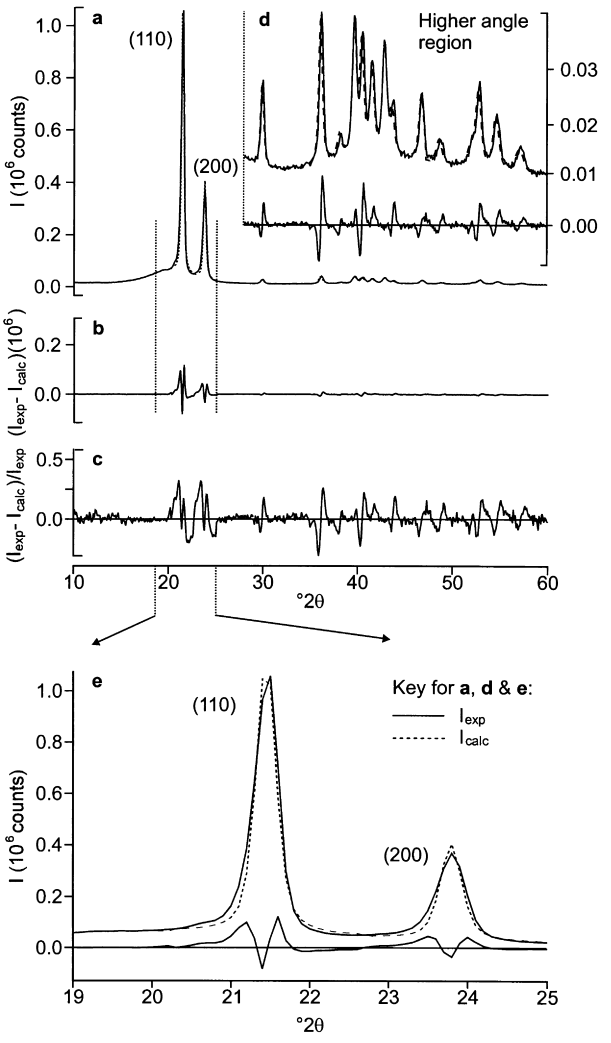

Fig. 1. Full (a) and magnified (d and e) views of the experimental and calculated wide-angle X-ray diffraction pattern from an unoriented sample of a branched polyethylene (5 methyl SCB/1000C), including absolute (b) and normalised (c) difference plots. The calculated pattern was determined by structural refinement of the whole pattern. (a) Experimental and calculated X-ray diffraction pattern across the full range of 10–60°2θ. (b) Absolute difference plot (exp. − calc). (c) Normalised difference plot, (exp. − calc.)/(exp.).

small extent in some samples with higher molecular weights.

2.3. X-ray diffraction from uniaxially oriented (fibre) samples

Fourteen of the 15 polyethylene grades were examined by X-ray diffraction in uniaxially oriented form. The fibre X-ray diffraction patterns were recorded in transmission mode using a novel fibre diffractometer based on a scanning CCD camera, recently designed and built in our laboratory [75,76]. CuKα radiation at 40 kV, 55 mA was used, with a germanium primary focusing monochromator. The principal attributes of the system were the ability to access all possible diffraction data from a fibre sample and to map the data into the fibre's cylindrically averaged reciprocal space to produce an undistorted section through reciprocal space. Each complete, composite fibre pattern (such as shown in Fig. 3) was mapped to a resolution of 0.002 Å^{-1} from approximately 200 images at different reciprocal space positions. Before mapping, each image was corrected for non-uniformity of detector response by dividing it by the image recorded under uniform illumination of the camera surface by X-ray radiation. In contrast to the unoriented diffraction data, the fibre thickness of only 0.3 mm meant that a correction for sample transparency was not necessary. Lorentz and polarisation corrections were also not applied.

Fitting and refinement of the patterns using Gaussian profiles was performed using the CCP13 suite of fibre diffraction software (Daresbury Laboratory). This software refined the cell parameters by fitting all peak positions to a single set of unit cell parameters and fitted the reflection intensities but did not include full structural refinement. Fourteen reflections were fitted: the first seven reflections along both the equator and the first layer line. It was only possible to fit a single wavelength component rather than separate CuKα_1 and CuKα_2 components but the broadness of the polyethylene reflections ensured that this was adequate. The amorphous scattering contribution was fitted as part of the background scattering.

3. Results

3.1. Unoriented (powder) samples

For unoriented samples of all grades, fitting to the whole pattern was dominated by the two intense, lowest angle reflections, (110) and (200), located between 21 and 24°2θ. A comparatively poor fit was obtained for all reflections, even for (110) and (200). This fitting is illustrated in Fig. 1 for a methyl-branched HDPE grade (*meth_5* in Table 1 of the previous paper [66]). The fit to (110) and (200) is shown magnified in Fig. 1e and reveals asymmetry in both reflections, especially in (110). In the fit to the higher angle reflections between 28 and 60°2θ, shown magnified in Fig. 1d, the peak shape is well matched, with little peak asymmetry, but all 16 reflections are shifted to lower angles than in the experimental data. This is revealed clearly by the difference plot of Fig. 1d. In the more highly branched grades the fitted higher angle reflections were also too broad.

In an attempt to overcome the dominating influence of the intense (110) and (200) reflections in the fitting procedure, fitting was restricted to the higher angle region, from 28 to 60°2θ, thereby excluding (110) and (200). This region of fit was then extended to include the (110) and (200) reflections, without allowing further refinement of the fitting parameters but merely extrapolating them to include the lower angle region 10–28°2θ. The result of this fitting approach is illustrated in Fig. 2, for the same unoriented methyl-branched

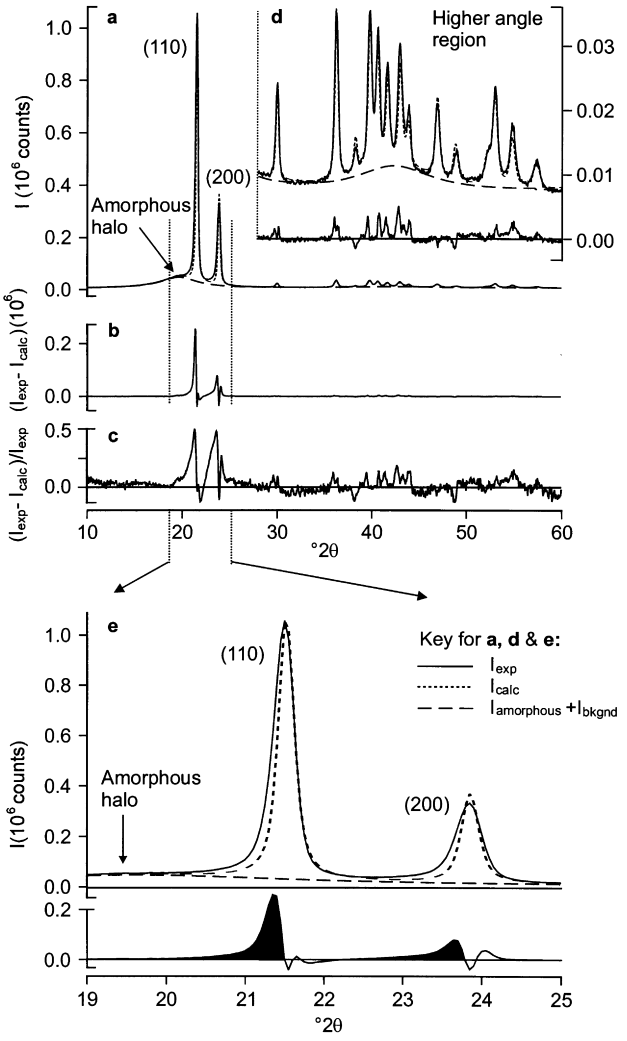

Fig. 2. Full (a) and magnified (d and e) views of the experimental and calculated wide-angle X-ray diffraction pattern from an unoriented sample of a branched polyethylene (5 methyl SCB/1000C), including absolute (b) and normalised (c) difference plots. The calculated pattern was determined by structural refinement of the higher angle region (28–60°2θ) and extrapolation of this fit without further refinement to include the (110) and (200) reflections in the lower angle region (10–28°2θ). (a) Experimental and calculated X-ray diffraction pattern across the full range of 10–60°2θ. The sum of the amorphous halo and background scattering contained within the calculated pattern is also shown. (b) Absolute difference plot (exp. − calc). (c) Normalised difference plot, (exp. − calc.)/(exp.). The two shaded portions of excess scattering near the (110) and (200) reflections in the magnified difference plot of (e) are seen to be broader than the calculated crystalline components and at slightly lower angles (corresponding to higher unit cell parameters).

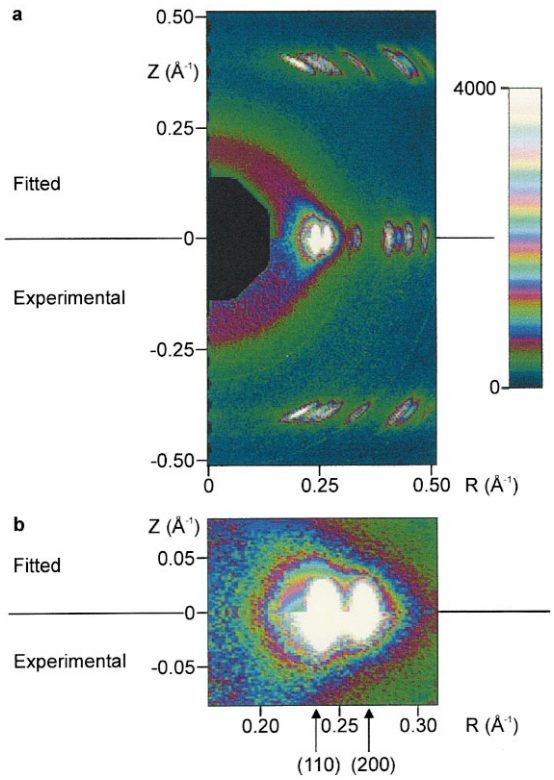

Fig. 3. Interpretation of the wide-angle X-ray diffraction pattern from a fibre sample of a branched polyethylene (the same grade as Fig. 1). (a) Experimental (lower quadrant) and fitted (upper quadrant) data. The fitted pattern was calculated by refinement to the 12 higher angle reflections in the range 28–60°2θ, and subsequent extrapolation of this fit to include the lower angle (110) and (200) reflections. The faint circles at $S = 0.32$ Å^{-1} and $S = 0.52$ Å^{-1}($S = \sqrt{(R^2 + Z^2)}$) are diffraction from silicon powder dusted onto the surface of the fibres for calibration purposes. The fit to the higher angle reflections is good but not to (110) and (200) (located approximately at $R = 0.25$, $Z = 0$ Å^{-1}). (b) Detail of the (110) and (200) reflections revealing additional scattering on the low angle side of the experimental data.

HDPE grade as used in Fig. 1. A good fit to the higher angle reflections is seen in Fig. 2d. The absence of sharp negative–positive fluctuations in the difference plot of Fig. 2d compared with Fig. 1d confirms the good agreement between experimental and calculated peak positions. Furthermore, the overall magnitude of the fluctuations is reduced: this is most clearly seen by comparing Fig. 2b and c with Fig. 1b and c. The fit to the lower angle region is shown magnified in Fig. 2e. This reveals that the fits to the (110) and (200) reflections were good on the high angle side. However, excess scattering in the experimental pattern is seen to remain unaccounted for on the low angle side of both reflections. Thus the experimental profiles of (110) and (200) in Fig. 2e appear unusually broad, asymmetric and having the peaks at too low an angle on the basis of the unit cell parameters calculated from the good fit to the 16 higher angle reflections. If refinement of the whole pattern was then attempted, the fitting regressed to that shown in Fig. 1: all the fitted peaks shifted to lower angle positions which clearly was not satisfactory for the higher angle reflections.

To summarise, it appeared that scattering contributions from the crystal structure of polyethylene could be fitted rather precisely across all the diffraction pattern reflections but excess scattering remained unaccounted for on the low angle side of the two strongest, lowest angle (110) and (200) reflections. This discrepancy was observed consistently in fitting to all grades.

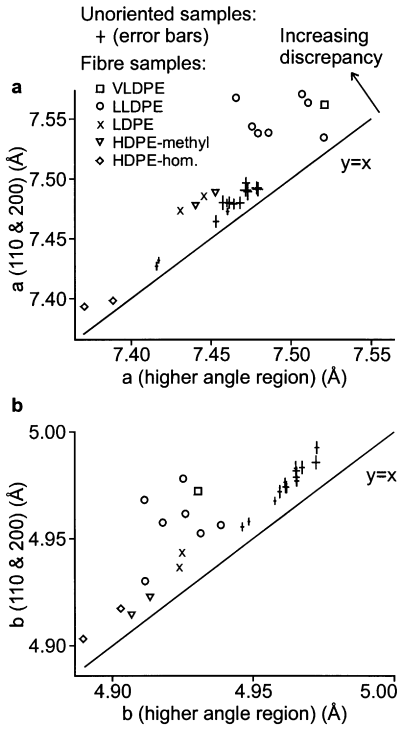

Fig. 4. Scatter plots of the *a* and *b* unit cell parameters refined from two different ranges of the X-ray diffraction pattern, for unoriented and fibre samples of 15 branched polyethylenes. The two ranges used for separate refinements were the (110) and (200) reflections (10–60°2θ), and 16 higher angle reflections (12 in the case of the fibre samples) (28–60°2θ). The solid lines labelled $y = x$ show where a(110 and 200) = a(higher angle region) and b(110 and 200) = b(higher angle region). The data-points should fall on these lines if there were no discrepancy between the two refinements; those data-points furthest from the lines show the greatest discrepancy. The fibre samples show a broader range of unit cell parameter values and also higher discrepancies than the unoriented samples; the largest discrepancies are seen for the more highly branched grades (LLDPE and VLDPE). The unoriented sample data-points are relatively tightly clustered, showing little variation in the magnitude of the discrepancy; for reasons of clarity they are not identified according to sample category.

3.2. Uniaxially oriented (fibre) samples

The same trends in diffraction pattern fitting as seen with the unoriented samples were also seen with the fibre samples of all grades. Fitting to the whole diffraction pattern was unsatisfactory whereas fitting only to the higher angle reflections followed by extrapolation of fit parameters to include (110) and (200) reflections could at least account for most of the scattered intensity. The fitting described here refers to the latter method.

The experimental diffraction pattern from a fibre sample of the same methyl-branched HDPE grade as shown in Figs. 1 and 2 is shown in Fig. 3. The pattern shows the intense pair of low angle equatorial reflections, (110) and (200), ($0.23\ \text{Å}^{-1} < R < 0.27\ \text{Å}^{-1}$, $Z = 0$) superimposed on a shallow amorphous halo ($S = 0.22\ \text{Å}^{-1}$, where $S^2 = R^2 + Z^2$). The higher angle region reflections are weaker in intensity than the strongest (110) reflection by a factor of at least 20. The calculated pattern was obtained by fitting to a back-to-front L-shaped section with ($0.32\ \text{Å}^{-1} < R < 0.52\ \text{Å}^{-1}$) and ($-0.32\ \text{Å}^{-1} < Z < 0.52\ \text{Å}^{-1}$) in the experimental pattern containing the 12 highest angle reflections. These fit parameters were then extrapolated to fit to the lower angle (110) and (200) pair of reflections, in a similar way as described above for the unoriented samples. By comparing the experimental and fitted patterns, the fit to the higher angle reflections is good (Fig. 3a) whilst the fit to the (110) and (200) reflections (Fig. 3b) is seen not to account for all of the scattered intensity. On the low angle side of both the (110) and (200) reflections, excess intensity remains (Fig. 3b), analogous to that seen for the unoriented sample in Fig. 2e.

3.3. The discrepancy in pattern fitting

The main discrepancy in fitting to different regions of the diffraction pattern as just described (either to the whole diffraction pattern or to the higher angle region followed by extrapolation to the lower angle region) was a difference in the calculated peak positions obtained and therefore a difference in the crystal unit cell parameters. The *a* and *b* unit cell parameters refined from fitting to the whole pattern (or just to the (110) and (200) reflections) showed a consistent enlargement over those refined from the higher angle reflections, in both unoriented and fibre sample forms. This is illustrated in Fig. 4. The unit cell *c* parameter can only be obtained from fitting to the higher angle reflections and so a discrepancy for this was not obtained. Fig. 4 shows that the size of the discrepancy in the *a* and *b* unit cell parameters was similar across all the unoriented samples. This was unlike the fibre samples which show considerably higher discrepancies in Fig. 4 than the unoriented samples. The extent of the discrepancy appears to be related to the grade of polyethylene, or in other words the branch content seems more influential than the branch type. The enlargement was greatest for the most highly branched grades, namely LLDPE and VLDPE. The unoriented sample data points are so heavily overlapped that they are not differentiated in symbol according to the grade of polyethylene; they are instead shown by error bars.

The relationship in the fibre samples between the discrepancy in unit cell parameters from refinement to the different regions of the diffraction pattern and the type of polyethylene is shown in more detail in Fig. 5. This shows the discrepancy as a function of branch content and the branch type is shown by the graph symbol used. In Fig. 5a, Δa is defined as the difference between the *a* unit cell parameter value obtained from refinement to the (110) and (200) reflections alone, and that obtained from refinement to the higher angle reflections: $\Delta a = a(110\&200) - a$(higher angle region). Equivalent definitions were applied to the *b* unit cell parameter values of each sample and the values of the product *ab*, representing the unit cell basal area

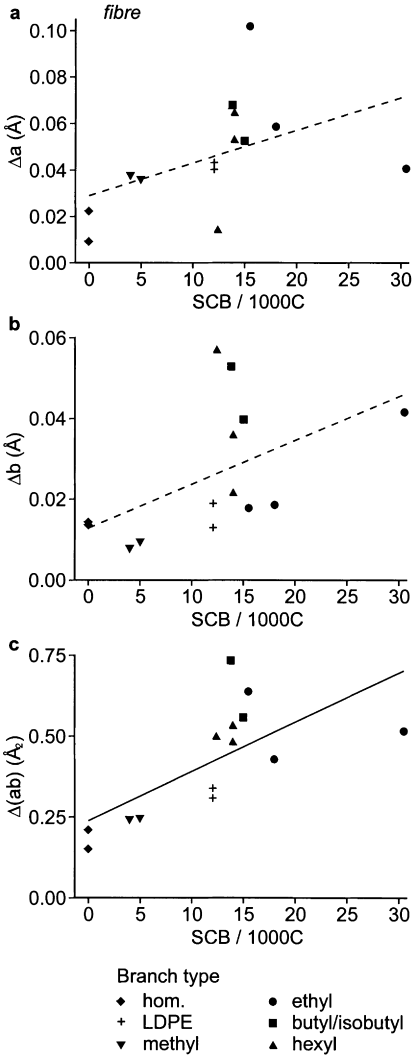

Fig. 5. The difference in unit cell parameters *a* (a) and *b* (b) and the unit cell basal area *ab* (c) from refinements to the (110) and (200) reflections and higher angle reflections (28–60°2θ) for the fibre samples, as a function of branch content. These differences, Δa and Δb, are the discrepancy values referred to in Fig. 4. The linear regressions are shown by a solid line if the slope was significantly different from zero ($P < 0.05$, *t*-test), dotted otherwise. The plots show an increase in the cell parameter differences as the sample branch content is raised. There is no clear effect of branch type.

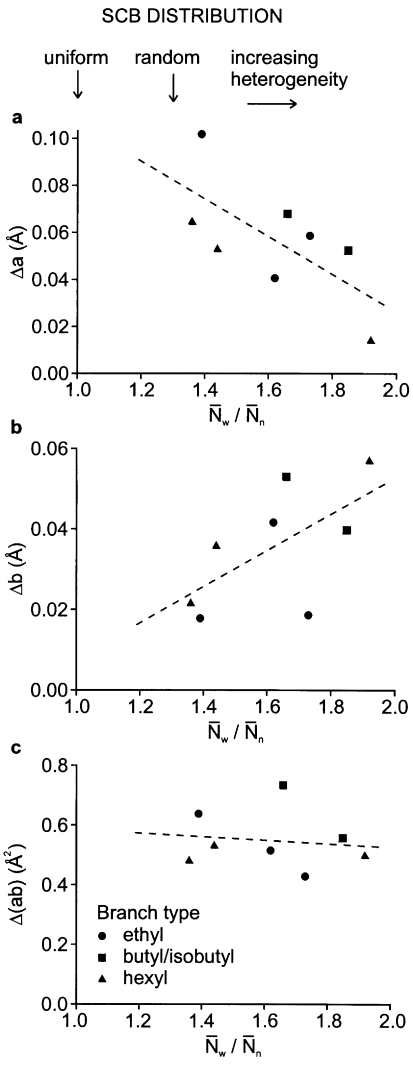

Fig. 6. The difference in unit cell parameters *a* (a) and *b* (b) and the unit cell basal area *ab* (c) from refinements to the (110) and (200) reflections and higher angle reflections (28–60°2θ) for the fibre samples, as a function of branch distribution. These differences, Δa and Δb, are the discrepancy values referred to in Fig. 4. The linear regressions are shown by a solid line if the slope was significantly different from zero ($P < 0.05$, *t*-test), dotted otherwise. The plots show an increase in the cell parameter differences with increasing heterogeneity in branch placement. There is no clear effect of branch type.

in Fig. 5b and c. An increase in the unit cell parameter discrepancy with increasing branch content is seen in Fig. 5 although there is considerable scatter in data-points, particularly for the cluster of more highly branched grades around 15 SCB/1000C (LLDPE grades). The increase reached significance, however, ($P < 0.05$, *t*-test on regression slope) for the *ab* product representing the unit cell basal area (Fig. 5c).

A relationship was also found between the discrepancy in cell parameters and the branch distribution of the polyethylene; this is shown in Fig. 6. The branch distribution was not known for all grades but Fig. 6 shows the seven LLDPE grades which had similar branch contents, in the range 15 ± 3 SCB/1000C, and for which the branch distribution $\bar{N}_w/\bar{N}_n$ parameter was known from TREF analysis. With increasing levels of heterogeneity in branch distribution, Δa appears to decrease whilst Δb appears to increase although the effects did not reach levels of significance. The net effect on $\Delta(ab)$ was negligible. This apparent dependence of Δa and Δb on branch distribution as well as branch content can account for much of the scatter in Fig. 4. The compensating effect shown in Fig. 6 of Δa and Δb depending on branch distribution in the opposite sense would also explain the reduced scatter of the cell basal area plot where the branch content trend reached significance (Fig. 5c).

4. Discussion

4.1. Interpretation of the discrepancy in pattern fitting

The inconsistency illustrated in Figs. 1 and 3 between fitting to the two lowest angle reflections, (110) and (200), and the higher angle reflections of polyethylene is believed to be genuine and not an artefact of the recording conditions nor refinement procedures, for the following reasons. (1) The discrepancy was found in all fifteen grades examined which covered a broad range of branch types (methyl to hexyl) and contents (0 to 31 SCB/1000C atoms, or up to 12 wt %). (2) The discrepancy was found in both unoriented and fibre samples. (3) The patterns from the two sample forms were recorded on two different diffractometers with different diffraction geometries (reflection and transmission modes for the unoriented and fibre forms, respectively) and analysed by two methods, one structural (the Rietveld method) and one non-structural (constrained fitting of peak positions via the unit cell parameters but not constrained fitting of intensities). (4) Goniometer alignment procedures and correction factors were applied, including a sample transparency correction for the reflection diffraction data [70], whose importance is rarely recognised for polymers. (5) The fitting to all higher angle reflections covering a range of 30°2θ was good and consistent in terms of peak shapes, positions and widths, and yet for the two lowest angle reflections, less than 10°2θ away, the fitting was poor in terms of peak shapes, positions and widths. (6) The difference between the unit cell parameters fitted to the two lowest angle reflections and the higher angle reflections was correlated with the branch content (Figs. 4 and 5) and furthermore branch distribution (Fig. 6). (7) Although anomalous in terms of reflection shape, position and width, the two lowest angle reflections still encompassed the crystalline scattering predicted from the higher angle reflections. (8) Finally, a similar discrepancy in the position of the (110) reflection has been briefly noted before [65]. Although it has never been mentioned in the literature within the context of a partially ordered component, the discrepancy found by Howard and Crist [65] will now be discussed and related to the discrepancies found in this paper.

Howard and Crist [65] studied the cell parameters of a series of model ethyl-branched polyethylenes, in oriented form. It was during their careful analysis of the X-ray diffraction pattern peak positions that they noted a discrepancy in the (110) reflection; a summary of their procedure follows. The polyethylenes were made into isotropic films, drawn to failure at room temperature (draw ratios in the range 1.0–7.3) and annealed under fixed length conditions at a temperature 20°C below the melting point for 2 h. Diffraction patterns from the drawn films along the equator and up the meridian to the (002) reflection at 75°2θ were recorded in symmetric transmission mode using CuKα radiation. A comprehensive series of correction factors were applied to the data, including for sample transparency. An unexpected feature of the study was that the experimental (110) interplanar spacing was consistently larger than that predicted from the *a* and *b* unit cell parameter values fitted to all the reflections i.e. as found in our study, the (110) reflection occurred at a lower angle than expected.

Regarding differences in methods, Howard and Crist [65] fitted unit cell parameters from reflections up to (002) at 75°2θ whereas we excluded the (110) and (200) reflections and fitted them from the 16 higher angle reflections in the range 28–60°2θ (12 reflections in the case of the fibre samples). As in our study, the discrepancy was highest for the most highly branched samples. Unlike our study, however, no discrepancy was noted in the position of the (200) reflection by Howard and Crist [65]. The discrepancy was argued to be genuine but it could not be explained. It was attributed tentatively to stacking faults although attempts to model the peak displacement from such faults were reported to have been unsuccessful and were not described.

We believe that the discrepancy noted by Howard and Crist [65] is commensurable with that reported here and there are several explanations for why a discrepancy in the position of (200) was not also noted by Howard and Crist [65]. From our data, the discrepancy in the (200) reflection peak position was nearly always smaller than for the (110) reflection. Also, the magnitude of the (110) peak position discrepancy reported here (maximum value 0.042 Å) tended to be larger than that reported by Howard and Crist [65] (maximum value 0.030 Å) and so probably the discrepancy in (200) peak position would have been smaller than that reported here and not detectable by Howard and Crist [65]. Furthermore the (200) reflection is weaker in intensity and broader than (110) and so is prone to larger errors in fitting. The cumulative effect of all these observations is that it is probably not significant and perhaps not surprising that Howard and Crist [65] reported a discrepancy in peak position only for the (110) reflection and not also for the (200) as found here.

A potential source of discrepancy between observed and expected peak positions in an X-ray diffraction pattern is the influence of the molecular transform, since an X-ray diffraction pattern is the product of the Fourier transform of the unit cell (the molecular transform) and the reciprocal lattice. It is conceivable that the molecular transform at the point sampled for the (110) and (200) reflections could be a point of high variation such that the slope of the molecular transform would be sufficient to cause a shift in the position of these reflections. This effect was investigated. First, an equatorial section through the molecular transform of polyethylene in cylindrically averaged reciprocal space was calculated. A diffraction pattern from one of the HDPE grades was then divided by this molecular transform section and the difference in peak positions of the equatorial (110) and (200) reflections caused by the slope of the molecular transform was calculated. The peak shifts found were

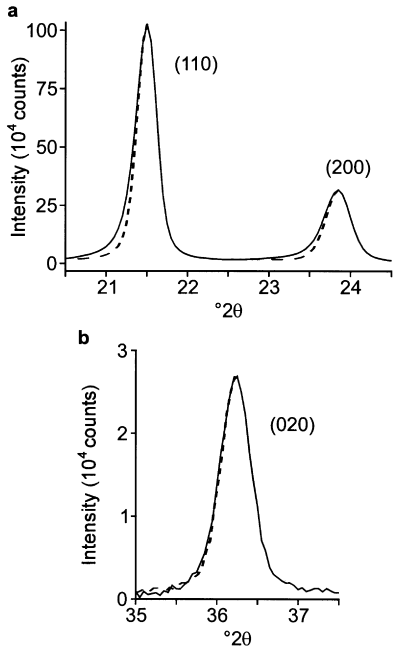

Fig. 7. Simple estimate of the degree of peak asymmetry in three reflections from the wide-angle X-ray diffraction pattern of an unoriented sample of a branched polyethylene (5 methyl SCB/1000C). (a) the (110) and (200) reflections and (b) the (020) reflection (from the higher angle region). The solid lines show the experimental data, after subtraction of amorphous and background scattering. The dashed lines show the high angle side of each reflection mirrored about the position of maximum intensity, as a simple test for the extent of peak asymmetry. Note: this figure should not be confused with Fig. 2d which shows instead the result of fitting a structural model to the X-ray diffraction pattern. The (020) reflection shows little asymmetry compared with the (110) and (200) reflections.

minimal ($<0.01°2\theta$) and below the resolution of the diffraction data collected. Thus the influence of the molecular transform cannot explain the peak shifts found experimentally.

We propose that the discrepancy found here between fitting to the (110) and (200) reflections and the higher angle reflections (and the discrepancy in (110) interplanar spacing noted by Howard and Crist [65]) using a two component model of crystalline and amorphous material can be explained by the presence of a third component of partial order. The (110) and (200) reflections are proposed to contain scattering from both crystalline and partially ordered regions whilst the higher angle reflections contain essentially only crystalline scattering: fitting to the 16 higher angle reflections (12 for the fibre samples) using the crystalline component was satisfactory across the whole range, $28–60°2\theta$.

The structure of the third component is likely to be based on that of the crystalline material because the scattering contributions from the two components were so closely associated. It therefore seems reasonable to suggest that the scattering may have originated from the surfaces of the crystallites, consistent with the interfacial component described earlier. Considerable evidence in support of this structural picture is available from a range of experimental techniques, as discussed earlier, but significantly not from the traditional structural investigation technique of wide-angle X-ray diffraction used here.

The third component is thought to have a lower degree of order than the crystalline component since its scattering contribution to the higher angle crystalline reflections was negligible. Such diminution in scattered intensity with angle can be interpreted by X-ray diffraction and paracrystallinity theory: as structural distortions and disorder are introduced into a crystalline material, the scattered intensity attenuates and broadens rapidly with scattering angle, appearing instead as part of the background [77]. For polyethylene, where the crystalline scattering is dominated in intensity by the two lowest angle reflections, the scattering contribution from such a partially ordered component to the weaker, higher angle crystalline reflections can be anticipated to be attenuated and broadened sufficiently so as to be merged with the background and irresolvable.

Qualitatively, it has been observed here from pattern fitting of the unoriented polyethylenes that the (110) and (200) reflections appeared more asymmetric in profile than the other reflections, with a broader tail on the low angle side (Fig. 2). Asymmetry of peak profiles is, however, a feature of the parafocusing conditions of Bragg–Brentano diffraction and an increase in peak asymmetry is expected at lower Bragg angles and is additionally enhanced by transparent, thick samples [70], although the effect of transparency had been corrected for here. Our evidence for a partially ordered component in polyethylene is based primarily upon the well-defined shift reported above in peak position for (110) and (200). It is mathematically difficult to demonstrate definitively a change in degree of peak asymmetry and it is not straightforward to ascertain whether such an increase in asymmetry is significant over that expected from the effects of diffraction geometry. Furthermore, fitting to (110) and (200) was hindered by overlap with the main amorphous halo, and several of the higher angle reflections were themselves overlapping. However, fitting to overlapping peaks in a diffraction pattern of a pure material where the structure is well known and where the data have high signal to noise ratio is relatively straightforward. The peaks were not fitted independently but according to one set of unit cell parameters, and there were sufficient non-overlapping peaks for unambiguous determination of the unit cell parameters. It is also worth noting that the symmetric pseudo-Voigt function proved adequate for fitting to all of the higher angle reflections with a single set of unit cell parameters, covering a range of over $30°2\theta$ ($28–60°2\theta$) and yet for the (110) and (200) reflections less than $10°2\theta$ away, a noticeable degree of asymmetry was observed.

4.2. Comparison of peak asymmetry between a polyethylene and a paraffin

As a check for the degree of peak asymmetry present

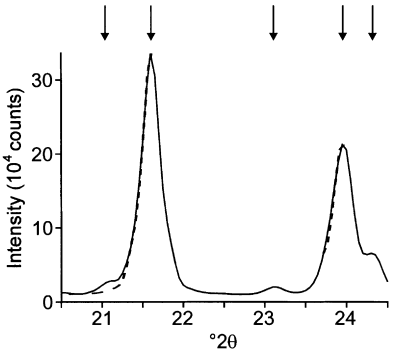

Fig. 8. Simple estimate of the degree of peak asymmetry in the wide-angle X-ray diffraction pattern of a paraffin, $C_{36}H_{74}$ (*n*-hexatriacontane). The region is the same as shown for polyethylene in Fig. 7a. The sample was made and the pattern was recorded under similar conditions to those used for the polyethylene, enabling direct comparison between the two patterns. Unlike polyethylene which shows two reflections in this region of 20.5 to 24.5°2θ (Fig. 7a), the paraffin shows an additional three reflections because it contains several different crystal structures; the arrows identify the five reflection positions [80]. The paraffin clearly shows very little if any peak asymmetry on the two main reflections, analogous to the higher angle (020) reflection of polyethylene but unlike the lower angle (110) and (200) polyethylene reflections.

here, the asymmetry in reflections from one of the unoriented samples of HDPE was estimated simply and qualitatively by mirroring the higher angle side of the reflection through the point of maximum intensity onto the lower angle side. This mirroring is shown in Fig. 7 by a dashed line and reveals the considerable asymmetry present in the (110) and (200) reflections, in contrast to the comparative symmetry of the next most intense reflection, (020) at 36°2θ. The amorphous and background scattering contributions were subtracted from each reflection prior to the asymmetry test.

As a further check of the apparent peak asymmetry in the (110) and (200) reflections of polyethylene, we also examined these reflections from a very low molecular weight polyethylene, $C_{36}H_{74}$ (*n*-hexatriacontane). The short, monodisperse chains of this paraffin are known to crystallise readily and extensively without chain folding [22,78] to produce essentially a fully crystalline polyethylene. A partially ordered component, if it exists at all in $C_{36}H_{74}$, must therefore represent no more than a tiny mass fraction of the paraffin. Any asymmetry present in the X-ray reflections from the paraffin is therefore expected to be slight and attributable largely to the effects of the X-ray diffraction geometry. This assumes that the asymmetry noted above in polyethylene was indeed caused predominantly by the proposed third component of partially ordered material rather than diffraction geometry, as indicated by Fig. 7. If the asymmetry seen in the polyethylenes were caused by the diffraction geometry, however, then similar degrees of peak asymmetry would be expected for the polyethenes and the paraffin. The $C_{36}H_{74}$ paraffin (molecular weight 5×10^2) was melt-crystallised to produce a sample with similar thickness (0.78 ± 0.03 mm) to the polyethylene sample of Fig. 7 (1.05 ± 0.03 mm). This was examined under the same X-ray diffraction conditions described earlier for the unoriented polyethylenes. The linear absorption coefficients of all polyethylenes and paraffins are very similar and so the same correction for sample transparency as for the polyethylenes was also applied to the paraffin data.

The chain structure and packing of polyethylene and $C_{36}H_{74}$ paraffin are very similar [79] although the diffraction patterns from such paraffins are more complex because end effects from the relatively short chains reduce the crystalline symmetry from that present in polyethylene, elongating the unit cell length parallel to the chain axis. Furthermore, $C_{36}H_{74}$ shows polymorphism, a common feature of paraffins. The diffraction pattern recorded from the $C_{36}H_{74}$ sample accordingly contained many more reflections than found in polyethylene. However, the underlying similarity in the structure of the paraffin to polyethylene was confirmed by the dominance of two strong interchain scattering reflections in the region just above 20°2θ, equivalent to the (110) and (200) reflections of polyethylene.

The same range 20.5–24.5°2θ as shown for polyethylene in Fig. 7 is shown for $C_{36}H_{74}$ in Fig. 8. It appears to contain five reflections although it was important to verify this before applying the asymmetry test in order to be aware of any overlapping peaks. Five peaks (with similar positions and relative intensities as those shown in Fig. 7) were also identified in this range by Reynhardt et al. [80] in their study of melt (and solution) crystallised $C_{36}H_{74}$ and assigned to one monoclinic and two orthorhombic structures. A weak shoulder on the high angle side of the main peak near 21°2θ from one of the orthorhombic structures [81] had been predicted by simulation but not identified experimentally [80]. Close examination of Fig. 8 reveals that a faint shoulder may be present at 21.8°2θ which if genuine will influence the asymmetry test but only to a slight extent. Having established the number and position of the reflections present in Fig. 8, the same procedure was applied to the two main reflections as applied to polyethylene in Fig. 7. The higher angle side of each reflection was mirrored through the point of maximum intensity onto the lower angle side, to estimate the extent of peak asymmetry present in the paraffin and is shown by the dashed line in Fig. 8. In spite of the two main reflections being partially obscured by overlap with weaker reflections, the general high degree of symmetry compared with the equivalent peaks in polyethylene (Fig. 7a) is clear. Figs. 7 and 8 are therefore consistent with the argument that unoriented polyethylenes contain partially ordered material, unlike paraffins.

4.3. Estimating the form of scattering from the partially ordered component

Evaluation of the exact nature of the partially ordered scattering was hindered by the heavy overlap of scattering from all three components (crystalline, amorphous and partially ordered) in the region of the (110) and (200) reflections, the scope in fitting to the broad amorphous halo and

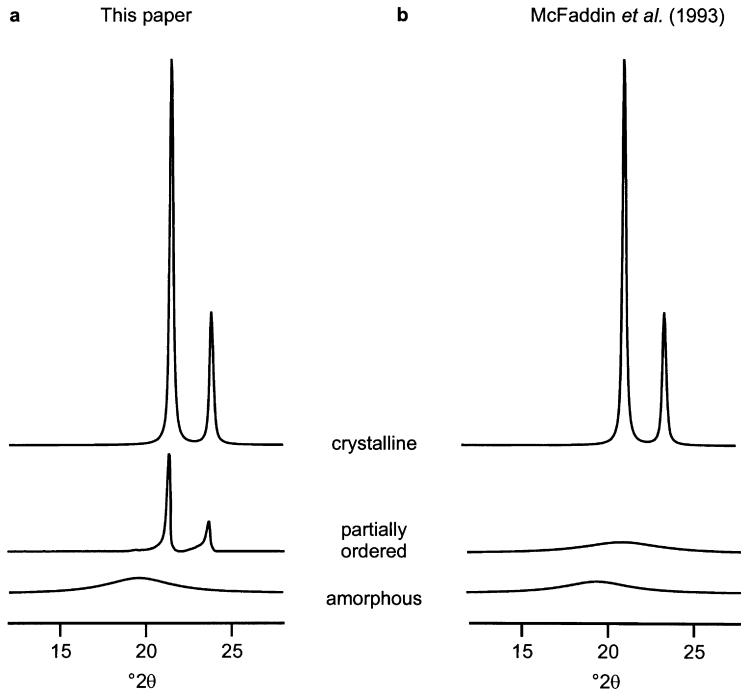

Fig. 9. A simple representation of the different nature of the partially ordered scattering contribution to the X-ray diffraction pattern of polyethylene proposed in this paper (a), and by McFaddin et al. (1993) [44] (b). The scaling between the three components in (a) and (b), the crystalline, partially ordered and amorphous scattering, should be used only as an approximate guide. We have found the partially ordered scattering to be more similar to the crystalline scattering than the amorphous scattering, contrary to McFaddin et al. (1993) [44].

the uncertainty in the temperature and scale factors of the crystalline component which are refined from the weak, higher angle reflections. These temperature and scale factors affect the proportion of the (110) and (200) reflection intensities attributed to the crystalline component. The extreme difference in intensities between the (110) and (200) reflections and the higher angle reflections where the temperature and scale factors were refined meant that small variations in the temperature factor which hardly affected the fit to the higher angle reflections had considerable influence on the predicted intensity of the (110) and (200) reflections. With the close association of the crystalline and partially ordered scattering, it was not found possible to extract a precise value of the crystalline temperature factor and thus the proportion of intensity attributable to crystalline material within the (110) and (200) reflections could not be determined accurately. However, in spite of the uncertainty in quantifying the partially ordered scattering, there was no uncertainty in the presence of such scattering in all samples.

An estimate of the form of scattering by the third component was obtained from the difference plot between the observed and calculated (crystalline plus amorphous) intensities and is reproduced from Fig. 2e (shaded portions) in Fig. 9a. This excess scattering shows two peaks, each broader and slightly lower in Bragg angle than the crystalline reflections. The profiles are highly asymmetric which indicates that the origin of the scattering cannot be characterised by a single set of structural parameters but rather that a range of degrees of order is likely to be present. For the (110) reflection at 21.5°2θ, the partially ordered scattering appears to extend to merge with the scattering of the amorphous halo at 19.6°2θ. The skew on the low angle side represents scattering from material with increasing levels of distortion and disorder and longer interchain spacings.

Fig. 9 illustrates the difference between our estimate of the scattering profile for the partially ordered component, taken from Fig. 2d(ii) and the estimate of McFaddin et al. (1993). The estimates are drawn approximately to scale with the crystalline and amorphous components. It is seen that our partially ordered scattering estimate is more similar to the crystalline scattering whereas the estimate of McFaddin et al. (1993) is more similar to the amorphous scattering.

4.4. The nature of the partially ordered material

The nature of the partially ordered material appears likely to depend on many factors, for example sample molecular weight, crystallisation conditions, heat treatment, the draw ratio used for fibres and temperature. Our study indicates that it is also affected by the branch content and distribution. Such a broad range of contributory factors would explain the variation in findings reported in the literature and the apparent lack of firm knowledge regarding the exact nature of the partially ordered material.

An experimental indication of the structural location of the partially ordered component was given by the fibre diffraction patterns. In a fibre pattern, diffraction from unoriented material appears as concentric circles each of

uniform intensity around the azimuth whilst diffraction from highly oriented material appears as short arcs. Fig. 3 shows that most of the scattering attributed to the third component was strongly aligned over the crystalline reflections although displaced to lower angles (larger lattice parameters). Thus the partially ordered material appears to share the same orientation and a similar extent of alignment as the crystalline material. These observations suggest that the two components are physically linked and the crystallite surfaces are an obvious location where such association could occur. The reasons for anticipating a partially ordered component at the crystallite surface are well known and were described in Section 1. For example, the chain packing at the surfaces of the crystals may be looser than within the bulk of the crystal. In addition, branches may be more easily accommodated at the crystal surfaces, particularly if the chains are less restrained in their packing. It has also not escaped notice that such scattering would be consistent with buried folds [82,83] within the crystallites which would gradually introduce the reduction in chain flux necessary at the crystallite surface for the transition to the amorphous component. Furthermore, it is conceivable that some of the partially ordered material could have originated from the localised loss of crystalline packing caused by increased levels of branching in a crystallite, particularly at the crystallite surfaces. The subject of inclusion of branches into the crystalline component and the influence of branch concentration is the subject of the third paper in this associated sequence [67].

5. Conclusions

A discrepancy concerning the peak positions in X-ray diffraction patterns from polyethylene has been found and interpreted. The discrepancy was found in all patterns recorded from a broad series of commercial grades, in both unoriented and uniaxially oriented sample forms. The extent of the discrepancy is most severe for the more highly branched polyethylenes and a relationship with branch distribution has also been found. The anomaly is attributed to the presence of a partially ordered component, found aligned with the crystalline component, in addition to the usual crystalline and amorphous components. Such a structural component has been proposed before from both theory and experimental work but intriguingly not until now from the traditional structural investigation technique of wide-angle X-ray diffraction.

Acknowledgements

The authors wish to thank BP Chemicals for the TREF analysis, Mary Vickers for discussions, Simon Hanna for advice concerning the fibre X-ray diffractometer, Chris Frye for supplying the materials and Brain Seymour, John Carter, Keith Page, Joe Ellis and Andrew Moss for technical support. The fibre diffraction patterns were analysed using the CCP13 suite of programs (CCLRC Daresbury Laboratory) and advice from Richard Denny and Gabriel Welsh is gratefully acknowledged. The molecular modelling was performed using the *Cerius*[2] software developed by Molecular Simulations Incorporated (Cambridge, UK). The work was supported by an EPSRC Research Studentship and CASE Award from BP Chemicals (AMEB).

References

[1] Schelten J, Ballard GH, Wignall GD, Longman G, Schmatz W. Polymer 1976;17:751–7.
[2] Mitchell GR, Lovell R, Windle AH. Polymer 1982;23:1273–85.
[3] Flory PJ. J Chem Phys 1949;17:223.
[4] Flory PJ. J Am Chem Soc 1962;84:2857–67.
[5] Flory PJ, Yoon DY, Dill KA. Macromolecules 1984;17:862–8.
[6] Mathur SC, Mattice WL. Macromolecules 1987;20:2165–7.
[7] Kumar SK, Yoon DY. Macromolecules 1989;22:3458–65.
[8] Ruland W. J Appl Crystallogr 1971;4:70–3.
[9] Vonk CG. J Appl Crystallogr 1973;6:81–6.
[10] Strobl GR, Hagedorn W. J Polym Sci (Phys) 1978;16:1181–93.
[11] Shen C, Peacock AJ, Alamo RG, Vickers TJ, Mandelkern L, Mann CK. Appl Spectrosc 1992;46:1226–30.
[12] Kitamaru R, Horii F, Murayama K. Macromolecules 1986;19:636–43.
[13] Cheng J, Fone M, Reddy VN, Schwartz KB, Fisher HP, Wunderlich B. J Polym Sci (Phys) 1994;32:2683–93.
[14] Voigt-Martin IG, Alamo R, Mandelkern L. J Polym Sci (Phys) 1986;24:1283–302.
[15] Kunz M, Moller M, Heinrich U-R, Cantow H-J. Makromol Chem Macromol Symp 1988;20/21:147–58.
[16] Gerum W, Hohne GWH, Wilke W. Macromol Chem Phys 1996;197:1691–712.
[17] Mandelkern L. Chemtracts (Macromol Chem) 1992;3:347–75.
[18] Naylor CC, Meier RJ, Kip BJ, Williams KPJ, Mason SM, Conroy N, Gerrard DL. Macromolecules 1995;28:2969–78.
[19] Mandelkern L, Alamo RG. Macromolecules 1995;28:2988–9.
[20] Naylor CC, Meier RJ, Kip BJ, Williams KPJ, Mason SM, Conroy N, Gerrard DL. Macromolecules 1995;28:8459.
[21] Frank FC. Faraday Discuss Chem Soc 1979;68:7–13.
[22] Hoffman JD, Miller RL. Polymer 1997;38:3151–212.
[23] Saito S, Moteki Y, Nakagawa M, Horii F, Kitamaru R. Macromolecules 1990;23:3256–60.
[24] Mandelkern L. Polym J 1985;17:337–50.
[25] Suzuki H, Grebowicz J, Winderlich B. Makromol Chem 1985; 186:1109–19.
[26] Popli R, Glotin M, Mandelkern L, Benson RS. J Polym Sci (Phys) 1984;22:407–48.
[27] Tanabe Y, Strobl GR, Fischer EW. Polymer 1986;27:1147–53.
[28] Packer KJ, Poplett IJF, Taylor MJ, Vickers ME, Whittaker AK, Williams KPJ. Makromol Chem, Macromol Symp 1990;34:161–70.
[29] Kitamaru R, Nakaoki T, Alamo RG, Mandelkern L. Macromolecules 1996;29:6847–52.
[30] Glotin M, Mandelkern L. Colloid Polym Sci 1982;260:182–92.
[31] Wang LH, Porter RS, Stidham HD, Hsu SL. Macromolecules 1991;24:5535–8.
[32] Vonk CG, Pijpers AP. J Polym Sci (Phys) 1985;23:2517–37.
[33] Schroter B, Posern A. Makromol Chem, Rapid Commun 1982;3:623–8.
[34] Packer KJ, Poplett IJF, Taylor MJ. J Chem Soc Faraday Trans 1988;84:3851–63.
[35] Kitamaru R, Horii F. Adv Polym Sci 1978;26:137–78.
[36] Russell KE, Wu G, Blake S, Heyding RD. Polymer 1992;33:951–7.

[37] Kitamaru R, Horii F, Zhu Q, Bassett DC, Olley RH. Polymer 1994;35:1171–81.
[38] Mutter R, Stille W, Strobl G. J Polym Sci (Phys) 1993;31:99–105.
[39] Alamo R, Domszy R, Mandelkern L. J Phys Chem 1984;88:6587–95.
[40] Alamo RG, Mandelkern L. Macromolecules 1989;22:1273–7.
[41] Mandelkern L, Prasad A, Alamo RG, Stack GM. Macromolecules 1990;23:3696–700.
[42] Bunn CW. Trans Faraday Soc 1939;35:482–91.
[43] Ruland W. Acta Crystallogr 1961;14:1180–5.
[44] McFaddin DC, Russell KE, Wu G, Heyding RD. J Polym Sci (Phys) 1993;31:175–83.
[45] Windle AH. In: Ward iM, editor. Developments in oriented polymers ILondon: Applied Science Publishers, 1982. p. 1–46.
[46] Bartczak Z, Galeski A, Argon AS, Cohen RE. Polymer 1996; 37:2113–23.
[47] Perkins WG, Porter RS. J Mater Sci 1977;12:2355–88.
[48] Ward IW. In: Ward IW, editor. Developments in oriented polymers I, London: Applied Science Publishers, 1982.
[49] Dupuis J, Legrand P, Seguelat R, Rietsch F. Polymer 1988;29:626–33.
[50] Lin L, Argon AS. J Mater Sci 1994;29:294.
[51] Kaji A, Ohta Y, Yasuda H, Murano M. Polym J 1990;22:455–62.
[52] Kaji A, Ohta Y, Yasuda H, Murano M. Polym J 1990;22:893–900.
[53] Tzou D-L, Huang T-H, Abhiraman AS, Desai P. Polymer 1992;33:426–8.
[54] Chen W, Fu Y, Wunderlich B, Cheng J. J Polym Sci (Phys) 1994;32:2661–6.
[55] Prasad K, Grubb DT. J Polym Sci (Phys) 1989;27:381–403.
[56] Moonen JAH, Roovers WAC, Meier RJ, Kip BJ. J Polym Sci (Phys) 1992;30:361–72.
[57] Fu Y, Busing WR, Jin Y, Affholter KA, Wunderlich B. Makromol Chem Phys 1994;195:803–22.
[58] Fu Y, Annis B, Boller A, Jin Y, Wunderlich B. J Polym Sci (Phys) 1994;32:2289–306.
[59] Fu Y, Chen W, Pyda M, Londono D, Annis B, Boller A, Habenschuss A, Cheng J, Wunderlich B. J Macromol Sci (Phys) 1996;B35:37–87.
[60] Auriemma F, Corradini P, De Rosa C, Guerra G, Petraccone V, Bianchi R, Di Dino G. Macromolecules 1992;25:2490–7.
[61] Nicholson TM, Davies GR, Ward IM. Polymer 1994;35:4259–62.
[62] Daubeny RdP, Bunn CW, Brown CJ. Proc R Soc London 1954;A226:531.
[63] Grubb DT, Prasad K. Macromolecules 1992;25:4574–82.
[64] Busing WR. Macromolecules 1990;23:4608–10.
[65] Howard PR, Crist B. J Polym Sci (Phys) 1989;27:2269–82.
[66] Baker AME, Windle AH. Polymer 2000;42:651–65.
[67] Baker AME, Windle AH. Polymer 2000;42:681–98.
[68] Bonner JG, Frye CJ, Capaccio G. Polymer 1993;34:3532–4.
[69] Frye CJ, BP Chemicals, Lavera, France. Personal communication, March 1996.
[70] Langford JI, Wilson AJC. J Sci Instrum 1962;39:581–5.
[71] Rietveld HM. J Appl Crystallogr 1969;2:65–71.
[72] Young RA. In: Young RA, editor. The Rietveld method, New York: Oxford University Press, 1993. p. 1–38.
[73] Wiles DB, Young RA. J Appl Crystallogr 1981;14:149–51.
[74] Dollase WA. J Appl Crystallogr 1986;19:267–72.
[75] Hanna S, Windle AH. J Appl Crystallogr 1995;28:673–89.
[76] Hanna S, Baker AME, Windle AH. Polymer 1998;39:2409–14.
[77] Hosemann R, Bagchi SN. Direct analysis of diffraction by matter. Amsterdam: North-Holland, 1962.
[78] Keller A, Organ SJ, Ungar G. Makromol Chem Macromol Symp 1991;48:93–102.
[79] Shearer HMM, Vand V. Acta Crystallogr 1956;9:379–84.
[80] Reynhardt EC, Fenrych J, Basson I. J Phys Condens Matter 1994;6:7605–16.
[81] Teare PW. Acta Crystallogr 1959;12:294–300.
[82] Keller A, Martuscelli E, Priest DJ, Udagawa Y. J Polym Sci (A2) 1971;9:1807–37.
[83] Windle AH. J Mater Sci 1975;10:252–68.